NASA TECHNICAL NOTE

NASA TN D-4770

ANALOG COMPUTER SIMULATION OF A DC ARC EMISSION SPECTROMETER CONTROL SYSTEM TO DEFINE REQUIREMENTS FOR OPTIMUM CONTROL

by Daniel J. Lesco

Lewis Research Center
Cleveland, Ohio

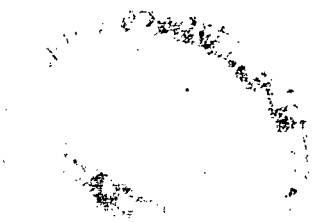

NATIONAL AERONAUTICS AND SPACE ADMINISTRATION • WASHINGTON, D. C. • AUGUST 1968

ANALOG COMPUTER SIMULATION OF A DC ARC EMISSION SPECTROMETER CONTROL SYSTEM TO DEFINE REQUIREMENTS FOR OPTIMUM CONTROL

By Daniel J. Lesco

Lewis Research Center
Cleveland, Ohio

NATIONAL AERONAUTICS AND SPACE ADMINISTRATION

For sale by the Clearinghouse for Federal Scientific and Technical Information
Springfield, Virginia 22151 – CFSTI price $3.00

ABSTRACT

The use of an analog computer in the simulation of a dc arc and its control system is described. The detailed model design is presented. Control parameters determined with the model are shown to be optimum with the real system. Repeatability of system control to a programmed input to ±1 percent is achieved for both the model and the real system. Data from the model and the arc system show close agreement except in some areas of arc instability.

ANALOG COMPUTER SIMULATION OF A DC ARC EMISSION SPECTROMETER CONTROL SYSTEM TO DEFINE REQUIREMENTS FOR OPTIMUM CONTROL

by Daniel J. Lesco

Lewis Research Center

SUMMARY

The use of an analog computer in the simulation of a dc arc and its control system is described. The detailed model design is presented. Control parameters determined with the model are shown to be optimum with the real system. Repeatability of system control to a programmed input to ±1 percent is achieved for both the model and the real system. Data from the model and the arc system show close agreement, except in some areas of arc instability.

INTRODUCTION

A new technique (ref. 1) in emission spectrochemical analysis being developed at the NASA Lewis Research Center requires control of the emission output of the static argon stabilized dc arc. Previously, constant-current control of the arc was used in spectrochemical analysis to improve the reproducibility of the sample vaporization, and, hence, the analytical precision. For further improvement in the precision of quantitative analysis, the use of a current control system based on the arc light intensity was deemed necessary. A control system (ref. 1) was incorporated to control the dc arc current such that the dispersed emission intensity received at a chosen photomultiplier (i. e., a selected element emission line) would follow a given programmed function of time repeatably to within 1 percent. This programming of the arc emission results in an indirect control of the arc temperature and plasma characteristics. Since the parameter of primary importance was the integral of the light intensity over the program time, transient errors of long duration could not be tolerated. However, difficulties were incurred in attempting to achieve stable operation of the control loop at the required gains.

The nonlinear and time-varying characteristics of the arc and its control system made theoretical analysis of the system very complex.

The use of analog computer simulation techniques appeared suitable and advantageous to the analysis of the control system. Nonlinear and time-varying parameters could be incorporated readily in the computer model. If successful simulation could be attained, the computer model might be useful in determining the control parameters for the system as a function of the electrodes to be used, the spectral line to be controlled, and the programmed input to be followed. Both time and cost might be saved over trial-and-error stabilization methods using numerous samples in the dc arc. Increased understanding of the arc control system and of the arc processes themselves might possibly be obtained by study of the simulator. Even without perfect simulation, areas could be singled out for further study by the elimination from consideration of the well-described characteristics of the arc system.

A study of the literature to determine if any analog simulation of dc arc emission had been reported was unfruitful. A literature search for mathematical models of the arc emission process was also unsuccessful. Studies have been made of the thermal and radiation characteristics of a static argon stabilized dc arc (ref. 2); but these studies are not directly applicable to spectral line emission. The emission intensity of a given element line is a complex process sensitive to temperature changes in the arc and, therefore, difficult to predict. The arc model used in this report was, therefore, based solely on experimental data obtained with the specific static argon dc arc used in the spectrochemical analysis.

This report describes the computer model used to simulate the arc and its control system and the information derived from the simulation. The use of simulation techniques required the experimental determination of the system functions. Approximations using experimental data were often required to permit a reasonably concise, analytical description of the system characteristics. With this knowledge of the arc and its control system mathematically stated, an analog computer model of the system was developed. The computer methods used and the results obtained are discussed in this report. Comparisons between the model and the real system were used to evaluate the simulation. Repeatability of control to a programmed input to ±1 percent was achieved. Parameters determining stability of the model were employed with the real system, noise effects were studied, and real system changes were incorporated based on the computer model results.

ARC CONTROL SYSTEM

The arc used in emission spectrochemical analysis at the Lewis Research Center is a static argon stabilized dc arc (ref. 3). The major components of the arc are shown in

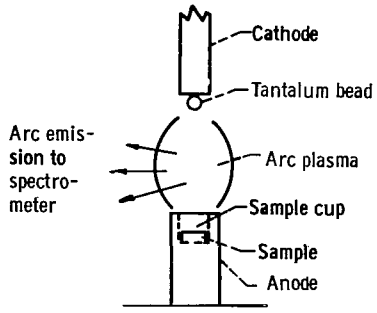

Figure 1. - Static argon stabilized dc arc.

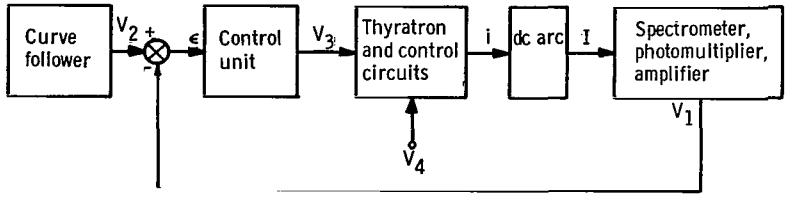

Figure 2. - Block diagram of dc arc and control system.

figure 1. The arc anode is fabricated with a cylindrical cup for holding the sample to be vaporized. The cathode is tipped with a tantalum bead. The emission from the arc gap is optically coupled to the spectrometer for analysis. The arc is contained in a chamber for control of the pressure and constituents of the arc atmosphere.

The control system (ref. 1) used with the dc arc achieves control of the arc emission intensity output by regulating the current to the arc. The controlled parameter is a selected spectral atom line of silver, Ag (350.2 nm). The block diagram of the arc control system is shown in figure 2. The intensity I, as detected at the Ag sensitive photomultiplier in the emission spectrometer, is proportional to the intensity of emission of the Ag in the arc gap. The electrometer amplifier converts the current output of the photomultiplier to a voltage output V_1 proportional to the Ag emission intensity. The curve follower provides a time-varying voltage V_2 as a program for emission intensity output to which V_1 is to be controlled. (The method for obtaining V_2 will be described in a later section.) Comparison of V_1 with the curve-follower voltage V_2 results in an error voltage $\epsilon = V_2 - V_1$. The control unit operates on ϵ, forming $K_1\epsilon$, $K_2(d\epsilon/dt)$, and $K_3 \int_0^t \epsilon \, dt$, whose summation is the control voltage V_3. The control voltage V_3 controls the thyratron current supply output i by phase shifting the thyratron grid signal. A positive change in V_3 increases the arc current, while a negative change decreases the current. Current changes in the arc are such as to minimize ϵ and thus cause V_1 to follow the desired program V_2. A constant voltage V_4 is used to provide a minimum arc current independent of ϵ.

The optimum values for K_1, K_2, and K_3 to achieve high gain control and stability are dependent on the arc function, the light measuring circuitry, and the current supply circuitry. The integral control voltage $K_3 \int_0^t \epsilon \, dt$ is used to maintain a steady-state error of zero. A control voltage $K(d\epsilon/dt)$ is used to provide system damping. To lessen the effects of high-frequency noise on the system response, the derivative signal is low-pass filtered.

DETERMINATION OF SYSTEM EQUATIONS

Analog computer simulation of the dc arc and the control system requires formulation of a mathematical model describing the system in terms of the function of its components.

The block diagram of the system (fig. 2) will be described by three functions experimentally determined from measurements on the arc and the associated electronics. A function $V_1(i, t)$ will be used to describe the voltage output corresponding to the intensity of the silver emission, with the arc current and time as the independent variables. The function $V_3(\epsilon, t)$ is the functional operation of the control unit acting on the error signal. Finally, $i(V_3, t)$ corresponds to the arc current as a function of the control unit output voltage and time.

Function $V_1(i, t)$

Description of $V_1(i, t)$ required experimental data of the steady-state and dynamic response of the Ag spectral atom line intensity to the arc current.

These experimental data showed that V_1 could be described by the equation

$$V_1(i, t) = f_{13}\left\{f_{12}\left[f_{11}(i, t)\right]\right\} \tag{1}$$

where this expression uses functional notation (i.e., f_{12} is a function of f_{11}, and f_{13} is a function of f_{12}). The function relating the arc emission intensity to the arc current is f_{11}. The function f_{12} describes the transient response of the emission intensity to changes in arc current, and f_{13} is the transient response of the electrometer amplifier.

The function f_{11} was determined by measuring the Ag emission intensity in terms of V_1 for several arc current values. The time dependence of f_{11} is a result of the arc temperature initially increasing at ignition and also of the decreasing amount of sample. For a constant initial sample size, therefore, f_{11} is a current-dependent, time-varying function. The variation in silver emission intensity from sample to sample (as large as 20 percent) made it necessary to average the results of several samples at each current level.

The peak light output during the vaporization of the sample was plotted as a function of arc current squared. Figure 3 shows this plot for two types of arc anode. In the region of interest (20 to 38 A of arc current) the data can be approximated by a linear function of the variable current squared. The peak Ag emission intensity for the anode

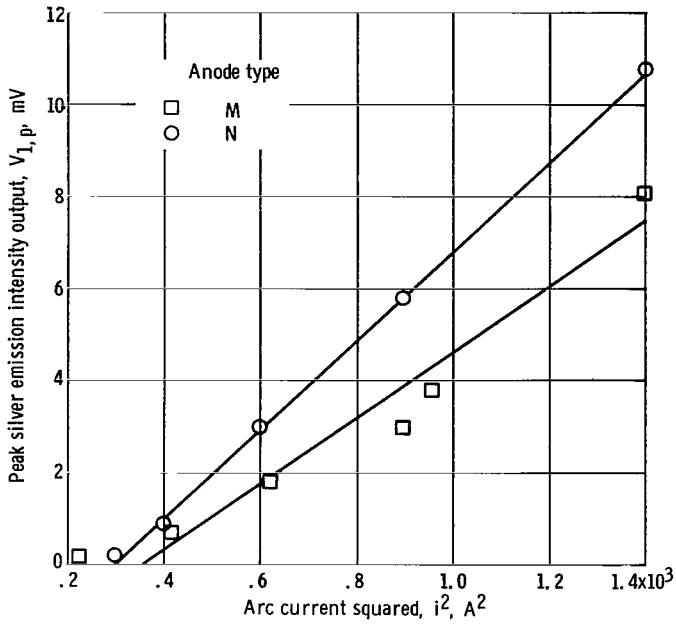

Figure 3. - Peak silver emission intensity as function of arc current.

TABLE I. - VALUES OF CONTROL SYSTEM CONSTANTS

Constant	Value
A	7×10^{-6} V/A^2
B	3.6×10^2 A^2
C	900 A^2
D	17 A
E	38 A
F	30 A/V
τ_1	1.4 sec
τ_2	0.2 sec
τ_3	0.1 sec

of primary interest in spectrochemical analysis (type M) is described by the function

$$V_{1,p} = A(i^2 - B) \tag{2}$$

(Table I lists the values of the constants used in this study.)

The Ag emission intensity output for 30 amperes constant current, with a 4-milligram sample of silver chloride (AgCl), is shown as a function of time in figure 4. If the curves obtained for other current levels are normalized along their time axes to the 30-ampere curve on the basis of the ratio of the current squared to 900 amperes squared, all of the normalized curves approximate in shape the 30-ampere Ag curve. (This is a reasonable result, since the integral of the Ag line intensity over the entire sample vaporization should be approximately constant for a constant sample size.) Therefore, the time function of the Ag light output can be described by

$$f_{11} = V_{1,p} f(t') \tag{3}$$

where

$$t' = \left(\frac{i^2}{C} t\right)$$

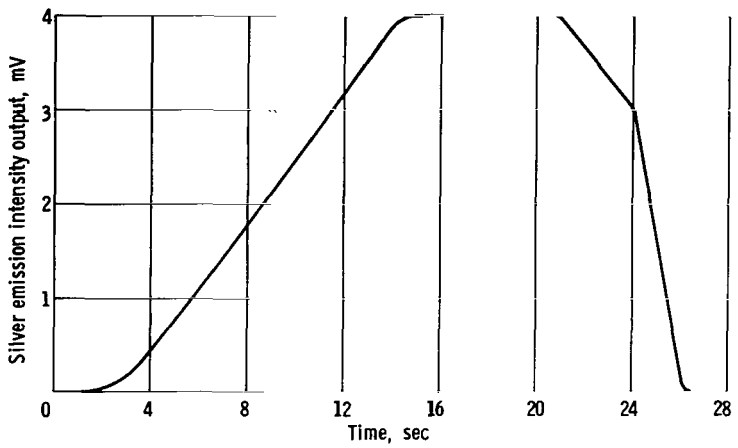

Figure 4. - Approximate silver emission intensity for 4-milligram sample of silver chloride at arc current of 30 amperes. (Test conditions from ref. 3.)

$$C = 900 \text{ amperes squared}$$

and $V_{1,p}f(t')$ is as shown in figure 4 for $i^2 = 900$. Therefore,

$$f_{11}(i, t) = A(i^2 - B)f\left(\frac{i^2}{C}t\right) \tag{4}$$

To obtain the transient response of the Ag light to current, step changes in current were applied to the arc during its operation and the Ag light response was measured. The Ag line was found to approximate a first-order (single time constant) response with a time constant τ_1 (where τ_1 was determined to be 1.4 sec for electrode type M). To within the ±20 percent error in measurements, τ_1 was found to be independent of i. Therefore, f_{12} can be described by the differential equation

$$\tau_1 \frac{\partial f_{12}}{\partial t} + f_{12} = f_{11} \tag{5}$$

The electrometer amplifier was known to contribute another first-order term with a time constant τ_2 (0.2 sec). Since the amplifier function is linear, its time response f_{13} can also be described by an independent first-order differential equation

$$\tau_2 \frac{\partial f_{13}}{\partial t} + f_{13} = f_{12} \tag{6}$$

The overall function $V_1(i, t)$ is obtained from equations (1), (4), (5), and (6) and can be described by the second-order differential equation

$$\tau_1\tau_2 \frac{\partial^2 V_1}{\partial t^2} + (\tau_1 + \tau_2) \frac{\partial V_1}{\partial t} + V_1 = A(i^2 - B) f\left(\frac{i^2}{C} t\right) \tag{7}$$

Function V_3

The function $V_3(\epsilon, t)$ for the control unit is related to the sum of the amplifier outputs generating the proportional, integral, and derivative signals by the equation

$$V_3(t) = K_1\epsilon + K_2 \frac{\partial \epsilon}{\partial t} + K_3 \int_0^t \epsilon \, dt \tag{8}$$

The values for the gains (K_1, K_2, and K_3) are separately adjustable.

Function i

The phase shifting and thyratron circuitry of the arc current supply are described by the function $i(V_3, t)$. A bias voltage V_4 (see fig. 2) is provided to maintain a minimum current level D of about 17 amperes. The maximum current E that can be supplied through the thyratron circuits is 38 amperes. The arc current supplied as a function of voltage V_3 is a nonlinear function for currents near the 38-ampere upper limit. However, the ampere-per-volt gain can be closely approximated by a linear relation and

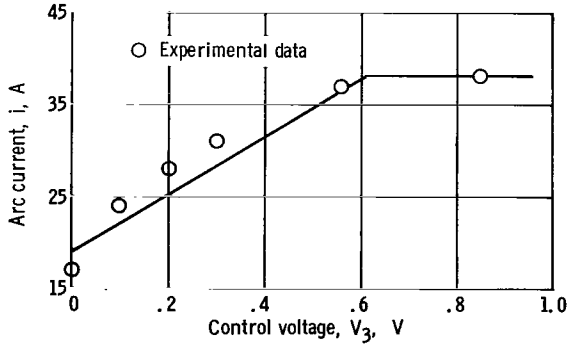

Figure 5. - Linear approximation of arc current as function of control voltage.

a limit at 38 amperes, as shown in figure 5. The linear slope F is 30 amperes per volt. With consideration of the bias current, the function is described by

$$i = D + FV_3 \qquad \left(\text{for } V_3 \leq \frac{E - D}{F}\right) \tag{9a}$$

$$i = E \qquad \left(\text{for } V_3 > \frac{E - D}{F}\right) \tag{9b}$$

The load inductance filtering the thyratron current waveform results in a first-order response of the current to the control voltage. The time constant $\tau_3 = 0.1$ second.

The function $i(V_3, t)$ may now be represented by the equations

$$\tau_3 \frac{\partial i}{\partial t} + i = D + FV_3 \qquad \left(\text{for } V_3 \leq \frac{E - D}{F}\right) \tag{10a}$$

$$i = E \qquad \left(\text{for } V_3 > \frac{E - D}{F}\right) \tag{10b}$$

This completes the mathematical model of the control system necessary for simulation techniques.

Effect of System Changes on Model

Although this simulation of the arc control system concentrates on the use of an Ag spectral line as its control parameter, it is entirely possible that other lines may be used in other applications. It was experimentally determined that the equation describing the arc emission does not have the same form for different element emission lines.

Preliminary data on the emission of a potassium K (404.7 nm) line showed that the arc function was of the form

$$V_1(t) = g_1(i, t) = g_{14}\left(g_{13}\left\{g_{12}\left[g_{11}(i, t)\right]\right\}\right)$$

where $g_{11}(i, t)$ describes the natural profile of the K emission, g_{14} involves the amplifier time constant, and g_{12} and g_{13} are two functions involving the transient response of the light emission process and are described by

$$\tau_1 \frac{\partial g_{12}}{\partial t} + g_{12} = g_{11}$$

$$\tau_1 \frac{\partial g_{12}}{\partial t} + a g_{12} = g_{13}$$

The response to a step change in arc current is a rapid increase to an output greater than the steady-state output followed by a first-order decay to the steady-state output.

Therefore, simulation of the system performance based on the control of other spectral lines would require significant changes in the system description. Experimental data on the response of a given spectral line to arc current at constant sample size must be obtained.

Similarly, as was illustrated by figure 3, the anode used in the dc arc affects the spectral emission of silver. Anode N achieved higher Ag emission intensity for a given current than did anode M. Though the transient response of the arc to current changes with anode N also exhibited a first-order response, the time constant was measured as 1.8 seconds, slightly greater than that for anode M.

These examples of changes in the system illustrate the need for experimental data to determine a model for the complex emission processes of the dc arc.

ANALOG SIMULATION OF DC ARC AND CONTROL SYSTEM

With a sufficient mathematical description of the arc and the control system completed, the simulation of the system by analog computer follows directly from the system equations (7), (8), (10), and

$$\epsilon = V_2 - V_1 \tag{11}$$

Equation (7) may be realized on an analog computer by the familiar method of solving for the highest derivative $\partial^2 V_1/\partial t^2$ and using computer integrators to form the lower order terms.

$$\frac{\partial^2 V_1}{\partial t^2} = -\frac{(\tau_1 + \tau_2)}{\tau_1 \tau_2} \frac{\partial V_1}{\partial t} - \frac{1}{\tau_1 \tau_2} V_1 + \frac{1}{\tau_1 \tau_2}\left[A(i^2 - B) f\left(\frac{i^2}{C} t\right)\right] \tag{12}$$

Equation (8), involving the variable i, is similarly solved for the highest order derivative.

$$\frac{\partial i}{\partial t} = -\frac{i}{\tau_3} + \frac{1}{\tau_3}(D + FV_3) \tag{13}$$

The functions $V_2(t)$ and $f(i^2t/C)$ are readily formed on an analog computer with diode function generators. The function generators present an output voltage as a function of an input voltage. If this input voltage is linearly increasing with time, the output voltage will be a function of time. To generate $f(i^2t/C)$, the input voltage to the function generator is the time integral of the term bi^2, where b is a constant adjusted such that a current of 30 amperes results in the function f(t) in real time. An increase in i^2 will proportionally increase the voltage ramp to the function generator, and, hence, decrease the time required to reach a given point in the output function.

The Ag emission intensity function which the output $V_1(t)$ is to follow is $V_2(t)$; this function is shown in figure 6. The steady-state level is the Ag emission intensity output generated by an arc current of 30 amperes. The function V_2 was chosen to control the Ag emission to values close to the natural constant current emission at 30 amperes. This restraint on V_2 was based on the advisability of reproducing arc emission characteristics for which previous experience in spectrochemical analysis had been obtained. The choice of V_2 also guaranteed that the analytical model of the arc would best fit the operating conditions with the control system, since the model was derived from experimental data at constant arc current. A deviation from the natural emission profile was programmed for the start of Ag emission.

The ramp portion of the curve precedes in time the natural profile of the Ag output at ignition of the arc at a current level of 30 amperes. This will result in a large cur-

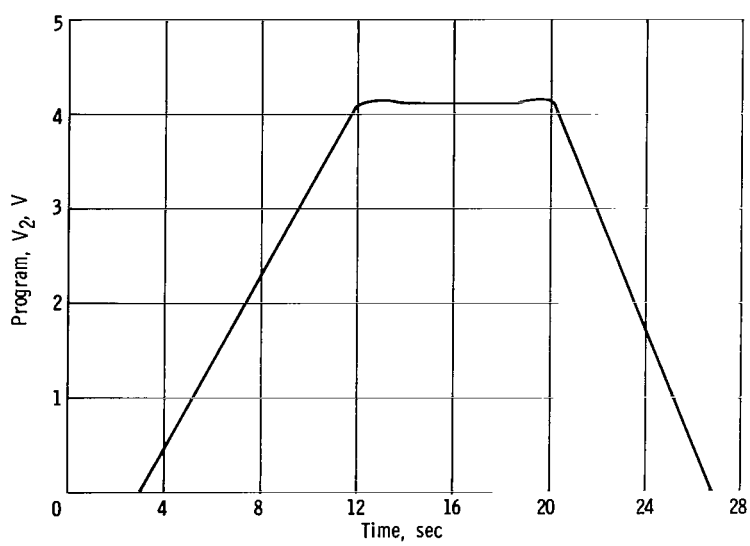

Figure 6. - Program for silver emission intensity output.

rent signal at the initial portion of the ramp to cause the earliest possible emission of the Ag at ignition. This criterion is conducive to the requirements for spectrochemical measurements of other volatile elements in the sample. It is also desirable, however, to limit the initial current surge below the maximum thyratron current, so as to maintain the current in control throughout the vaporization of the entire sample.

The slight nonlinearities in the shape of $V_2(t)$ at maximum voltage (as shown in fig. 6) are a result of limitations in the use of diode function generators for connecting linear segments of a function. The effects on the model response are negligible.

The analog computer simulation of the control system was achieved on a 10-volt full-scale analog computer. Since the time parameters involved were suitable for real time programming, no time scaling was necessary. However, voltage amplitude scaling was necessary in order to observe the variables of interest: $V_1(t)$, $V_2(t)$, $\epsilon(t)$, and $i(t)$. Table II lists the computer variables and magnitudes, and the computer scale factors.

TABLE II. - COMPUTER VARIABLES AND UNITS

Variable	Maximum value	Scale factor
$V_1(t)$	10 mV	1 V/mV
$V_2(t)$	10 mV	1 V/mV
$i(t)$	38 A	0.1 V/A
$i^2(t)$	1444 A^2	0.001 V/A^2

Rewriting equation (13), and expressions for $i(t)$ and $V_3(t)$, for the computer variables results in the computer equations

$$10^3 \frac{\partial^2 V_1}{\partial t^2} = - \frac{(\tau_1 + \tau_2)}{\tau_1 \tau_2} \left(10^3 \frac{\partial V_1}{\partial t} \right) - \frac{1}{\tau_1 \tau_2} (10^3 V_1) + \frac{1}{\tau_1 \tau_2} \left\{ 10^6 \left[Af\left(\frac{i^2}{C} t \right) \right] \left[10^{-3} (i^2 - B) \right] \right\} \tag{14}$$

$$10^{-1} \frac{\partial i}{\partial t} = - \frac{10^{-1} i}{\tau_3} + \frac{1}{\tau_3} \left[10^{-1} (D + F V_3) \right] \tag{15}$$

$$V_3(t) = \frac{K_1}{10^3} (10^3 \epsilon) + \frac{K_2}{10^3} \left(10^3 \frac{\partial \epsilon}{\partial t} \right) + \frac{K_3}{10^3} \int_0^t 10^3 \epsilon \, dt \tag{16}$$

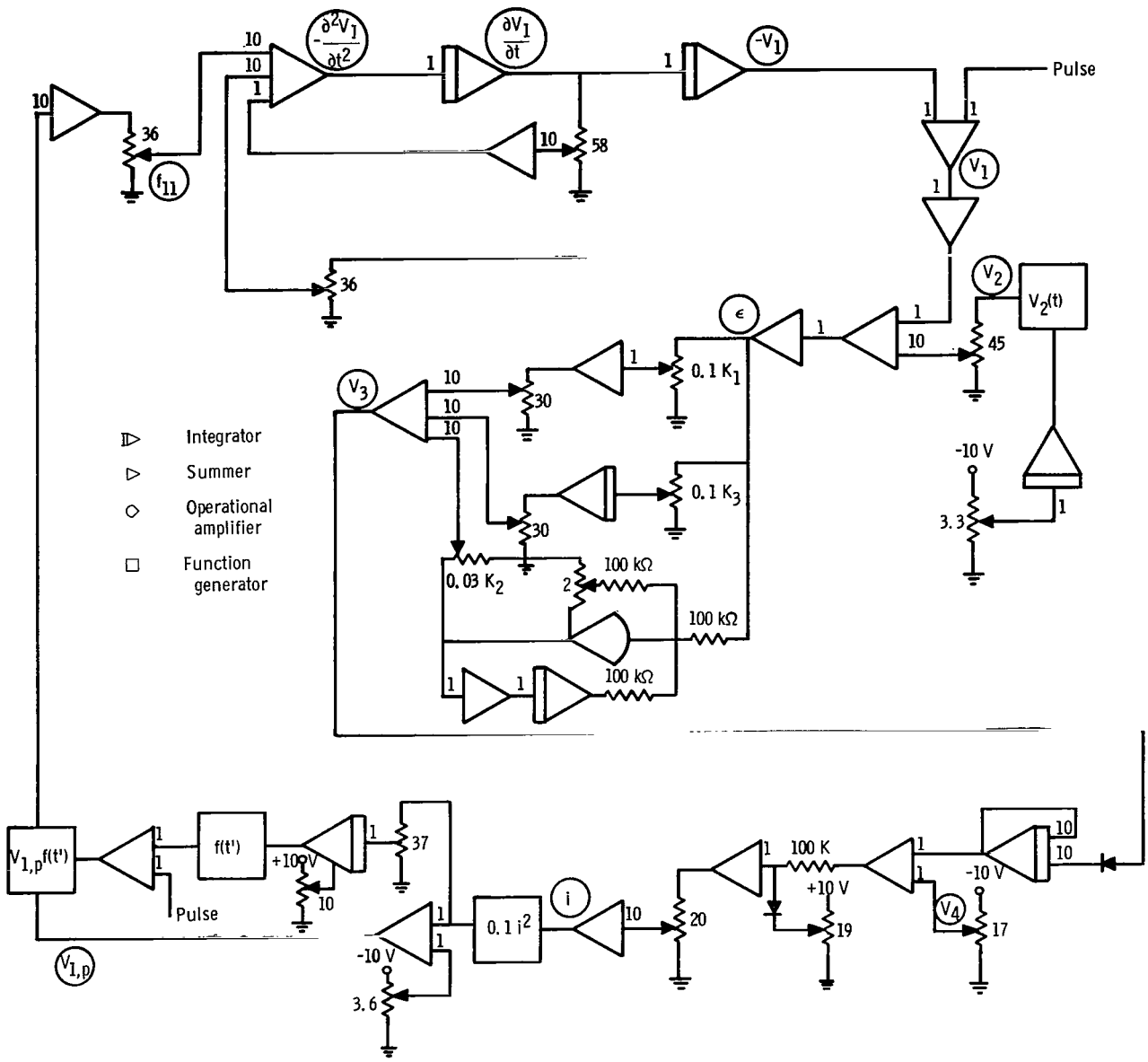

Figure 7. - Analog computer model for dc arc and control system.

Figure 7 shows the complete computer simulation of equations (14), (15), and (16). The computer variables are shown in the diagram where they occur, although the amplitude scaling is not explicitly labeled. The function generators are labeled as to the function programmed. The symbols used for integrator, summer, operational amplifier (no internal feedback), and function generators are listed in the key. The numbers on the input lines to the integrators and summers represent the gain for the respective inputs (i. e., gain of 10 or 1).

The differentiating circuit provides an approximate first derivative of the error signal by

$$V_{out}(t) = K_2 \frac{\partial \epsilon}{\partial t} - a \frac{\partial V_{out}}{\partial t} \qquad (17)$$

where a is a variable set at 0. 02 to limit the derivative signal at frequencies above 8 hertz, thereby lessening the effect of high-frequency noise on the circuit response.

The potentiometer settings are shown in the diagram (fig. 7) as percent of signal transmitted, with the gain potentiometers labeled as a function of proportional, integral, or derivative gain.

Provision for the simulation of arc noise is provided at the inputs labeled "Pulse." The natural profile of the Ag emission line as a function of time, shown in figure 4, is an average curve which does not show the higher frequency noise pulses encountered in the arc. This noise is simulated by the manual pulses provided by external circuitry. The pulse rise time is in the millisecond range, while the decay time constant is 0. 1 second.

RESULTS AND DISCUSSION

The analog computer simulator was used to determine the optimum proportional, integral, and derivative gains for the real system. Study of the simulator operation resulted in improvement of the real system design. Comparisons of simulator and real system responses provided information on the accuracy of the arc model.

Gain parameters exhibiting stable control on the model were used with the real system and comparisons were made by using the real system and the model responses to an emission intensity program. The bases of comparison are the system stability, the emission-intensity waveform, and the arc-current waveform. A strict comparison in waveforms is limited by the sample-to-sample variations in the Ag emission intensity for equal quantities of AgCl and by limitations in accurately simulating the random fluctuations in emission intensity. It was noted earlier that the magnitude of the emission

intensity output for constant arc current was found to vary from sample to sample by as much as 20 percent.

Simulator Response

The simulator characteristics were studied for various magnitudes and interrelations of proportional, integral, and derivative gains. The proportional gain was increased in steps until only minor improvements in control were obtained or until unstable control occurred. The integral gain was adjusted to reduce the initial error as rapidly as possible without excessive overshoot of the emission intensity program and without causing the arc current to reach the current limit.

The effect of integral gain is illustrated by figure 8. The integral gain K_3 for curve 2 is twice that for curve 1 (1000:500). The emission intensity output V_1, the programmed input V_2, the arc current i, the natural profile function f(t'), and the error voltage ϵ are displayed as recorded in real time. The differences in i and ϵ for curves 1 and 2 are to be noted. The increase in K_3 for curve 2 results in a higher initial surge in i at t = 5 seconds, resulting in a decrease in ϵ to zero at about t = 6 seconds and a subsequent overshoot (negative error signal) until t = 9 seconds. For curve 1, the error does not decrease to zero as rapidly, but no significant overshoot occurs. (Although the computer runs are continued to about t = 24 sec, sample vaporization in the real system would be terminated at about 22 sec; this is the time at which V_2 starts to decrease.)

The derivative gain was adjusted to provide system damping for minimization of overshoot and oscillation in the system waveforms for ideal conditions (as in fig. 8) and also for noise disturbances applied to the system.

Figure 8 shows a slight anomaly in the waveforms f(t') and V_1. During the time $t < 4$ seconds, V_1 remains zero while f(t') slowly increases because of the minimum bias current of 17 amperes. The voltage V_1 is zero because the bias current is insufficient to result in a positive value for $V_{1,p}$ as determined by the linear approximation in figure 3. The real dc arc does exhibit a slight Ag emission for minimum arc current, but the integral of this value of emission for a 4-second period is negligible compared to the total Ag emission.

Since arc noise disturbances in the form of spikes in emission intensity were always present in the real system operation, the computer studies were concentrated on determining the effects of noise as a function of the control gains. Noise pulses were applied at f(t') and at V_1 (see fig. 7). The pulses at f(t') were to simulate discontinuities in the vaporization of the AgCl at the arc anode. Inconsistencies in the form or purity of the AgCl could conceivably cause this effect. Pulses were applied at V_1 to simulate

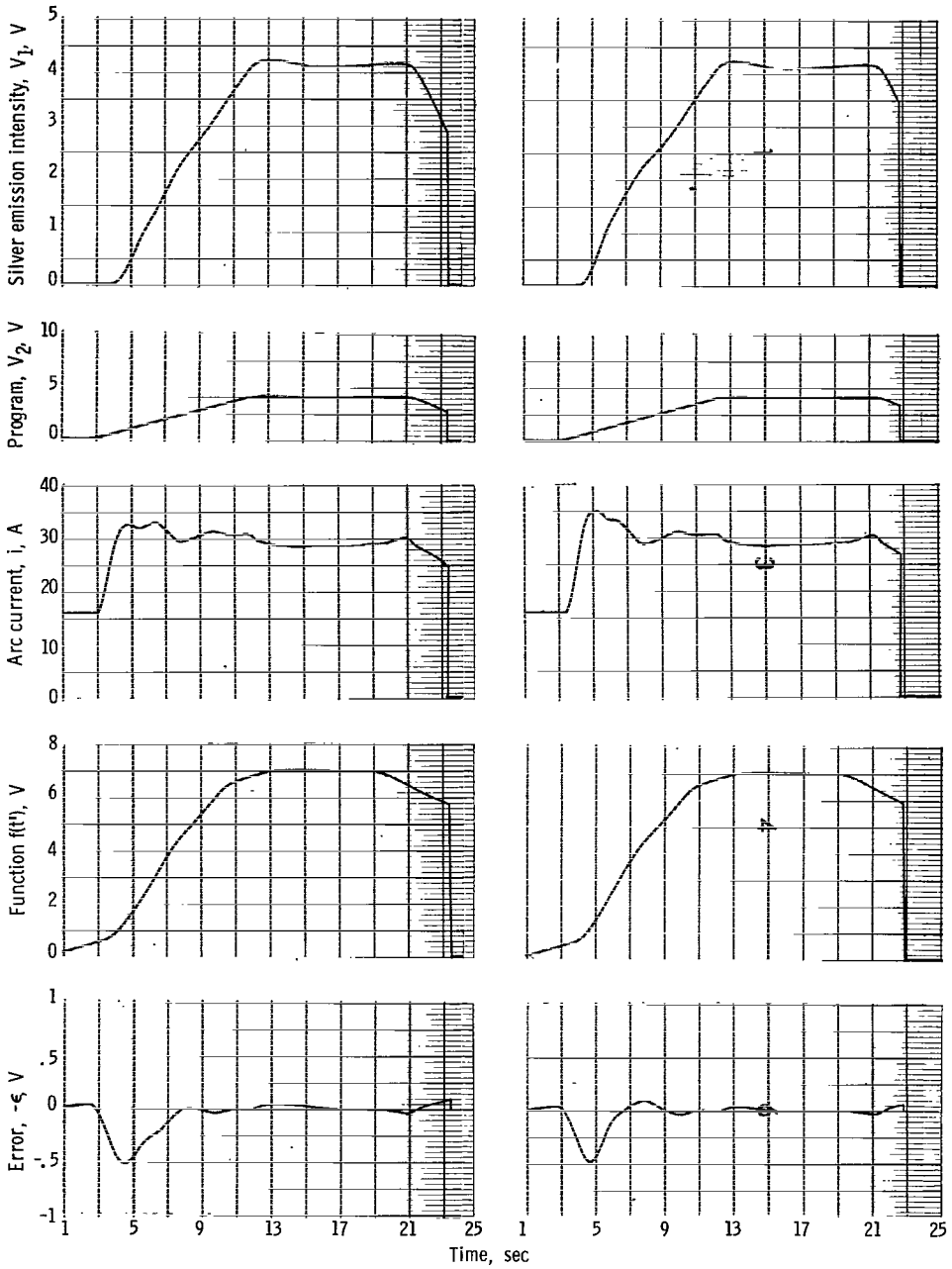

(a) Curve 1. Integral gain, K_3, 500.

(b) Curve 2. Integral gain, K_3, 1000.

Figure 8. - Effect of change in integral gain on simulator response. Proportional gain, K_1, 1000; derivative gain, K_2, 300.

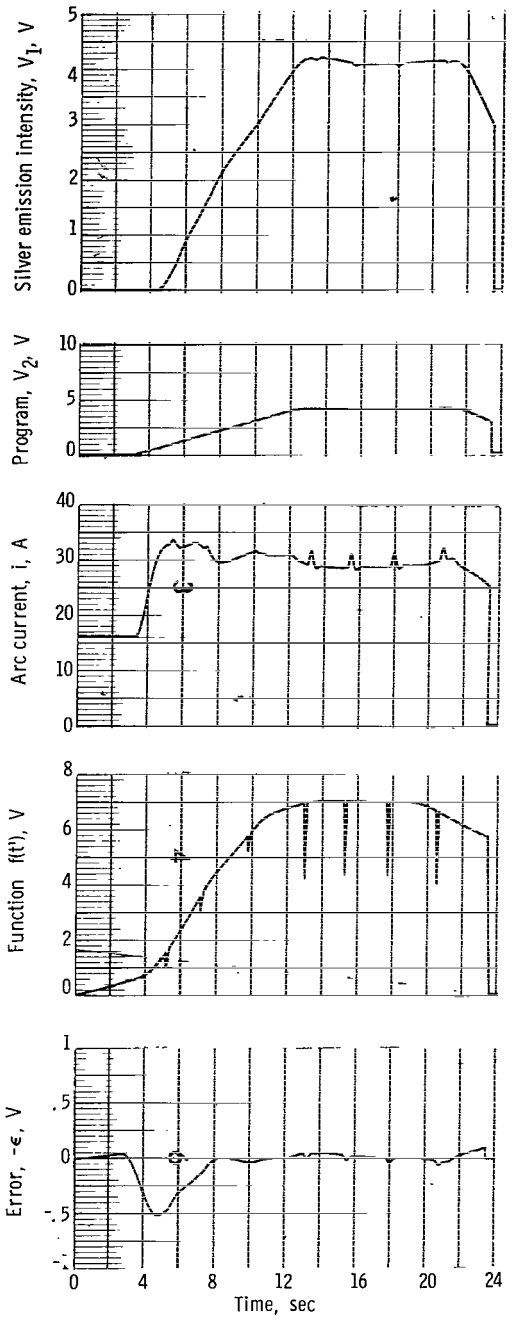

Figure 9. - Model response to noise pulses applied at f(t'), with optimum derivative gain. Proportional gain, K_1, 1000; derivative gain, K_2, 300; integral gain, K_3, 500.

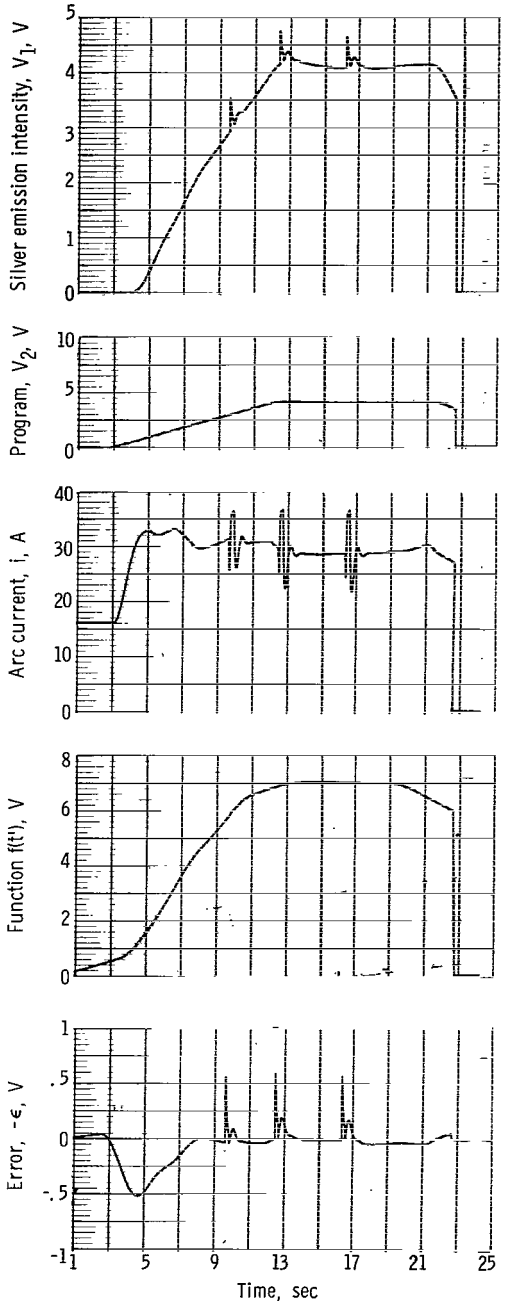

Figure 10. - Model response to noise pulses applied at V_1, with optimum derivative gain. Proportional gain, K_1, 1000; derivative gain, K_2, 300; integral gain, K_3, 500.

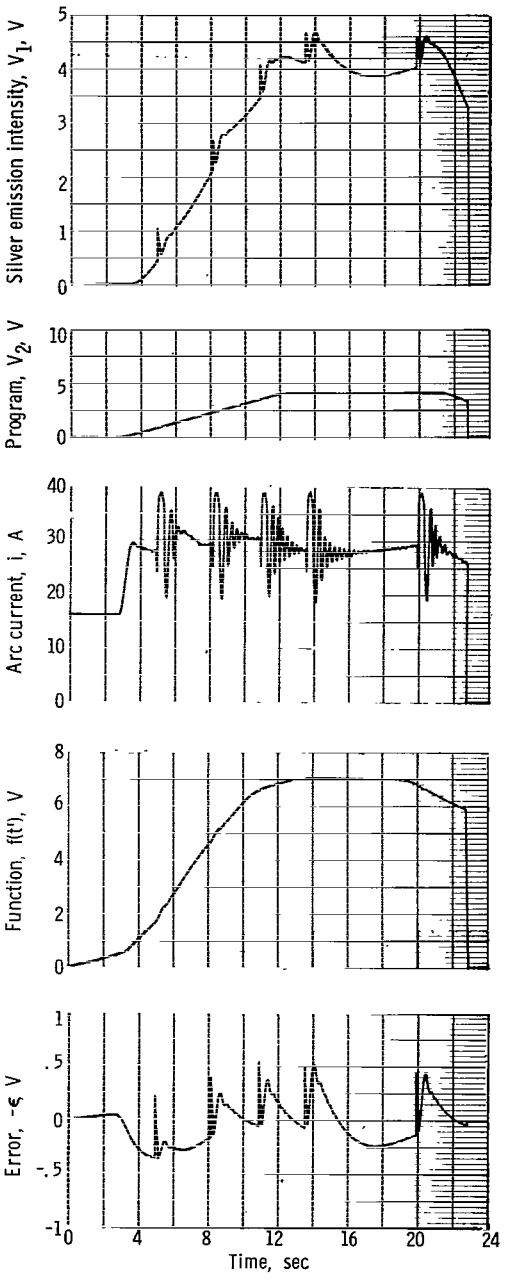

Figure 11. - Model response to noise pulses applied at V_1, with high derivative gain. Proportional gain, K_1, 1000; derivative gain, K_2, 1500; integral gain, K_3, 500.

system operation under noise conditions representing changes in the arc chamber or in the spectrometer and electronics which would affect the Ag emission intensity output directly. These changes might be the result of arc temperature fluctuations, minor plasma displacements, or electronic noise.

Figure 9 shows the operation of the simulated arc system with noise disturbances at f(t'), with optimum integral and derivative gains for the proportional gain of 1000. After the initial transient error, control to within ±1 percent of program is achieved. The transient effects of the current changes required to correct for the noise disturbances are negligible.

Figure 10 illustrates the system operation for disturbances at V_1. These disturbances are more disruptive to system control than were pulses at f(t'). The control gains are adjusted for minimal transient effects - the transients reduce to near zero within 1 second after the disturbance. The effect of a large change in derivative gain (1500) for disturbances at V_1 is shown in figure 11. The current oscillations result in large (10 percent) errors of several seconds duration.

Comparisons of Model and Real System

The use of optimum control gain parameters, derived from the model study, generally resulted in stable, optimum control with the real system. For proportional and integral gains of 1000 and 500, respectively, stable arc control was achieved with a derivative gain of 300. The real system response under these gain conditions is illustrated by figure 12. Control to the program to within 1 percent is achieved, with the exception of the repeatable initial lag. The current waveform is similar to that achieved on the simulator (as in fig. 8). The emission intensity disturbance halfway up the ramp portion of the program is corrected by a current change whose transient decays within about 2 seconds. (In fig. 12, because of the recording pen offsets, the current trace leads the emission intensity output trace by 1 sec. For that reason, the output disturbance does not exactly coincide in time with the current response as recorded in the figure.)

Although simulator response did not vary appreciably (with $K_1 = 1000$ and $K_3 = 500$) for a range of derivative gains of ±30 to 40 percent, this was not the case with the real system. Variation of the derivative gain of more than 20 percent from optimum resulted in unstable operation of the control system. It appears that instabilities in the dc arc are triggered by current oscillations which result from noise disturbances. This discrepancy between the model and real system responses will be discussed later.

Comparisons of the arc system and its model were also made at higher proportional and integral gains. In general, the derivative gains for optimum damping were about equal. For proportional gains of 5000 on the model, the band of derivative gains for

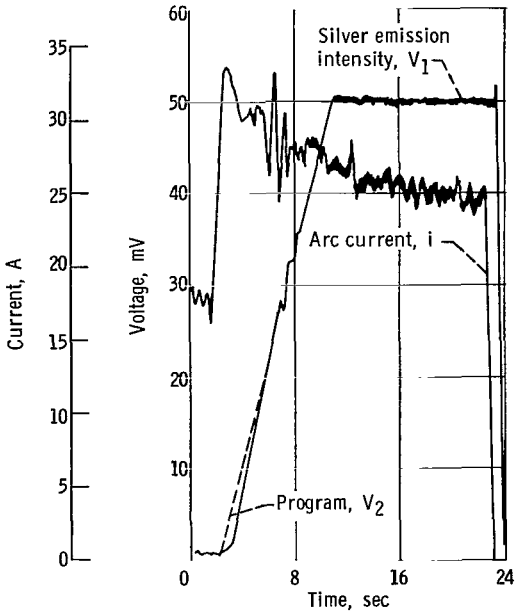

Figure 12. - Real system response to input program.

stable response to noise disturbances was about 20 percent, and even the best responses exhibited transient oscillations, as shown in figure 13. It can be noted in the figure that although the initial transient error for $t < 4$ seconds has been reduced, the high control gains have caused the initial current surge to reach the current limit at 38 amperes. During this time of about 1 second duration, the current control was saturated and could not respond to noise disturbances. Although stable control of the dc arc could also be attained at this control gain, no significant improvement in Ag emission control was achieved because of more pronounced noise transient effects. Stable operation was not achieved at proportional gains of 10 000 or above for either the model or the real system.

Some improvement in the dc arc control system resulted from studies on the computer model. Measurements of the derivative control gain for the system prior to simulation showed that the derivative gain decreased as a first-order function above a frequency of 3 hertz. Study of the model responses showed that improvements in system stability could be obtained if the derivative gain corner frequency was extended to 8 hertz. A change was made in the real system to incorporate this characteristic. The result was a significant improvement in real system stability.

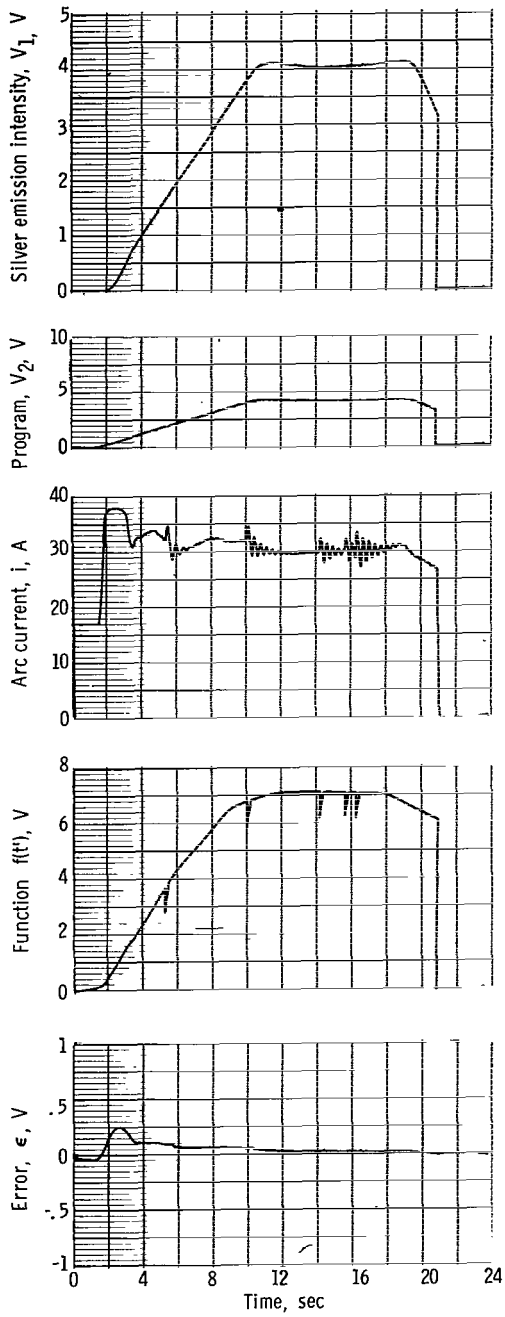

Figure 13. - Model response with proportional gain K_3 of 5000. Derivative gain, K_2, 900; integral gain, K_3, 500.

Real System Instabilities

The analog simulator exhibited limitations in accurately reproducing arc instabilities which can be disruptive to control of the emission intensity.

The foremost example of the model limitations involved arc instabilities related to the alinement of the arc electrodes. This little-understood phenomenon became evident during several of the initial sample vaporizations with the real arc system. With gain and arc operating conditions for which stable arc operation had been obtained regularly, control of the Ag emission line became unstable. These instabilities at first seemed to be related to the cathodes used (ref. 3), since insertion of a new cathode often resulted in control oscillations. However, it was then determined that reinsertion of previously stable cathodes did not necessarily guarantee stable control. It was determined experimentally in open-loop operation that there were no apparent changes in the arc function f_{11} for stable or unstable cathodes.

An explanation of this phenomenon was arrived at through subsequent testing. It was determined that a slight misalinement of the axes of the arc cathode and anode resulted in stable operation. Since the cathode construction techniques (ref. 3) often resulted in slightly unsymmetrical cathodes, reinsertion of a cathode did not necessarily place it in the same position relative to the anode. When care was taken to insert the cathode in a predetermined orientation, stable control of the arc was achieved.

A possible explanation of the dependence of arc stability on electrode positioning followed from visual observation of the plasma streaming between the arc electrodes. For the slight misalinement condition of the electrodes, the plasma streaming from cathode to anode appeared to achieve a stable, circular flow pattern. With the cathode tip closely alined with the anode axis, however, the plasma flow pattern impinged on the anode directly, the pattern was irregular, and arc instabilities occurred.

It was noted earlier that the range of derivative gains for stable control of the real system was narrower than the range of optimum gains for the model. For proportional gains of about 5000, large changes in derivative gain from the optimum value were necessary to cause instability of the model. The real arc appeared to be more susceptible to current oscillations caused by noise disturbances. Once unstable, the emission intensity oscillations were of larger magnitude than would be expected on the basis of the computer model studies.

Further studies of the arc function under various conditions of plasma flow and for external and internal disturbances are necessary to provide sufficient information to better characterize the arc emission processes for computer simulation.

General Observations

The computer simulation of the dc arc and the control system were used in this study as a tool to determine optimum gain parameters for control of the Ag emission intensity. It has been noted earlier that changes in the element emission line being controlled or in the arc electrodes necessarily change the analytical description of the system. Further studies with simulation techniques might be helpful in determining what characteristics of the parts of the system result in optimum control. Also, the use of various input programs could readily be investigated with the model for optimization of control with consideration for the requirements of spectrochemical analysis. These uses for the analog simulator would all be enhanced by improvements in the analytical description of the arc emission processes.

SUMMARY OF RESULTS

An analog simulation of a dc arc and its control system was developed and used to determine optimum control gain parameters for the real system. The analytical model for the arc emission process was derived from experimental data. The following are the results from the study of the analog model and from comparisons between the model and real system responses:

1. The model was used to obtain control gain parameters for stable operation of the real dc arc system.
2. The effects of noise disturbances on the control of the model emission intensity were studied.
3. The analytical model of the dc arc was shown to be a function of the dc arc parameters, including the controlled element emission line and the arc anode.
4. The model of the dc arc emission process was found to have some limitations in simulating instabilities in the arc.

Lewis Research Center,
National Aeronautics and Space Administration,
Cleveland, Ohio, April 23, 1968,
129-03-14-04-22.

REFERENCES

1. Gordon, William A.: A Servocontroller for Programming Sample Vaporization in Direct-Current Arc Spectrochemical Analysis. NASA TN D-4769, 1968.
2. Wutzke, S. A.; Cremers, C. J.; and Eckert, E. R. G.: The Thermal Analysis of Anode and Cathode Regimes in an Electric Arc Column. Rep. HTL-TR-56, Univ. Minnesota (NASA CR-58082), Aug. 1963.
3. Gordon, William A.: Stabilization of DC Arcs in Static Argon Atmospheres for Use in Spectrochemical Analysis. NASA TN D-4236, 1967.

NASA-Langley, 1968 —— 8

NATIONAL AERONAUTICS AND SPACE ADMINISTRATION
WASHINGTON, D.C. 20546

OFFICIAL BUSINESS

FIRST CLASS MAIL

POSTAGE AND FEES PAID
NATIONAL AERONAUTICS AND
SPACE ADMINISTRATION

POSTMASTER: If Undeliverable (Section 158 Postal Manual) Do Not Return

"The aeronautical and space activities of the United States shall be conducted so as to contribute . . . to the expansion of human knowledge of phenomena in the atmosphere and space. The Administration shall provide for the widest practicable and appropriate dissemination of information concerning its activities and the results thereof."

—NATIONAL AERONAUTICS AND SPACE ACT OF 1958

NASA SCIENTIFIC AND TECHNICAL PUBLICATIONS

TECHNICAL REPORTS: Scientific and technical information considered important, complete, and a lasting contribution to existing knowledge.

TECHNICAL NOTES: Information less broad in scope but nevertheless of importance as a contribution to existing knowledge.

TECHNICAL MEMORANDUMS: Information receiving limited distribution because of preliminary data, security classification, or other reasons.

CONTRACTOR REPORTS: Scientific and technical information generated under a NASA contract or grant and considered an important contribution to existing knowledge.

TECHNICAL TRANSLATIONS: Information published in a foreign language considered to merit NASA distribution in English.

SPECIAL PUBLICATIONS: Information derived from or of value to NASA activities. Publications include conference proceedings, monographs, data compilations, handbooks, sourcebooks, and special bibliographies.

TECHNOLOGY UTILIZATION PUBLICATIONS: Information on technology used by NASA that may be of particular interest in commercial and other non-aerospace applications. Publications include Tech Briefs, Technology Utilization Reports and Notes, and Technology Surveys.

Details on the availability of these publications may be obtained from:

SCIENTIFIC AND TECHNICAL INFORMATION DIVISION

NATIONAL AERONAUTICS AND SPACE ADMINISTRATION

Washington, D.C. 20546